Kinetics and identities of extracellular peptidases in subsurface sediments of the White Oak River Estuary, NC

Running title: Extracellular enzymes in subsurface sediments

Andrew D. Steen[a,b,#], Richard T. Kevorkian[a], Jordan T. Bird[a,*], Nina Dombrowski[c,†], Brett J. Baker[c], Shane M. Hagen[b,‡], Katherine H. Mulligan[b,d,§], Jenna M. Schmidt[b], Austen T. Webber[a], Taylor Royalty[b], Marc J. Alperin[e]

[a]Department of Microbiology, University of Tennessee, Knoxville, Tennessee, USA

[b]Department of Earth and Planetary Sciences, University of Tennessee, Knoxville, Tennessee, USA

[c]Department of Marine Science, University of Texas-Austin, Marine Science Institute, Port Aransas, Texas, USA

[d]Department of Biology, University of North Carolina at Chapel Hill, Knoxville, Tennessee, USA

[e]Department of Marine Sciences, University of North Carolina at Chapel Hill, USA

[#]Corresponding author. email: asteen1@utk.edu

mail: Strong Hall 601, 1621 Cumberland Avenue, Knoxville, TN 37996-1410

tel: (865) 974-4014, fax: (865) 974 2638

22 *Present address: Indiana University Bloomington, Indiana, USA

23 [†]Present address: Royal NIOZ, Texel, The Netherlands

24 [‡]Present address: University of Tennessee Health Science Center, Memphis, TN, USA

25 [§]Present address: East Carolina Brody School of Medicine, Greeneville, NC

Abstract

Anoxic subsurface sediments contain communities of heterotrophic microorganisms that metabolize organic carbon at extraordinarily slow rates. In order to assess the mechanisms by which subsurface microorganisms access detrital sedimentary organic matter, we measured kinetics of a range of extracellular peptidases in anoxic sediments of the White Oak River estuary, NC. Nine distinct peptidase substrates were enzymatically hydrolyzed at all depths. Potential peptidase activities (V_{max}) decreased with increasing sediment depth, although V_{max} expressed on a per cell basis was approximately the same at all depths. Half-saturation constants (K_m) decreased with depth, indicating peptidases that functioned more efficiently at low substrate concentrations. Potential activities of extracellular peptidases acting on molecules that are enriched in degraded organic matter (D-phenylalanine and L-ornithine) increased relative to enzymes that act on L-phenylalanine, further suggesting microbial community adaptation to access degraded organic matter. Nineteen classes of predicted, exported peptidases were identified in genomic data from the same site, of which genes for class C25 (gingipain-like) peptidases represented more than 40% at each depth. Methionine aminopeptidases, zinc carboxypeptidases, and class S24-like peptidases, which are involved in single-stranded DNA repair, were also abundant. These results suggest a subsurface heterotrophic microbial community that primarily accesses low-quality detrital organic matter via a diverse suite of well-adapted extracellular enzymes.

IMPORTANCE

Burial of organic carbon in marine and estuarine sediments represents a long-term sink for atmospheric carbon dioxide. Globally, ~40% of organic carbon burial occurs in anoxic estuaries and deltaic systems. However, the ultimate controls on the amount of organic matter that is buried in sediments, versus oxidized into CO_2, are poorly constrained. Here we used a combination of enzyme assays and metagenomic analysis to identify how subsurface microbial communities catalyze the first step of proteinaceous organic carbon degradation. Our results show that microbial communities in deeper sediments are adapted to access molecules characteristic of degraded organic matter, suggesting that those heterotrophs are adapted to life in the subsurface.

58 ## Introduction

59 A large fraction of the microorganisms in subsurface sediments are heterotrophs
60 that metabolize aged, microbially altered organic matter (1–3). These communities'
61 metabolisms can be more than a million-fold more slower than cells in culture (1, 4). A
62 recent meta-analysis showed that only about 12% of cells in marine sediments belonged
63 to cultured species, while 27% belong to phyla that contain no cultured representatives
64 (5). Consequently, the mechanisms by which these microorganisms access detrital
65 organic matter are poorly understood (6).

66 In surface environments, where organic carbon metabolism is relatively rapid,
67 heterotrophic microorganisms gain energy by metabolizing a combination of small
68 molecules (<600-1000 Da), which can be taken up directly via general uptake porins (7)
69 and macromolecules, which must be broken down outside of the cell by extracellular
70 enzymes. Most freshly-produced organic matter is macromolecular, and large molecules
71 tend to be more bioavailable than small ones (8), so the nature and activity of
72 extracellular enzymes present in surface environments is a major control on the rate of
73 microbial carbon oxidation in such environments.

74 It is not clear whether microbial extracellular enzymes play the same role in
75 subsurface sediments. It is conceivable that macromolecules are broken down primarily
76 by non-enzymatic mechanisms in sediments. For instance, in soils, MnO_4 catalyzes the
77 depolymerization of proteins without requiring enzymes. Certain bacterial species can
78 use TonB-dependant transporters to transport polysaccharides that are substantially larger
79 than 600 Da into the periplasm (although enzymatic hydrolysis is still required prior to

uptke into the cytoplasm; 9). Furthermore, some of the unique aspects of subsurface sediments suggest that extracellular enzymes might not be an effective strategy to obtain carbon or energy. In order for the production of extracellular enzymes to be part of a viable metabolic strategy, each enzyme must, over its lifetime, provide the cell with at least as much carbon or energy as was required to synthesize the enzyme (10–12). In subsurface sediments, where cell division times may be on the order of decades to millenia, enzyme lifetimes would need to be correspondingly longer to remain 'profitable'. Since enzyme lifetimes are finite, there must exist a community metabolic rate below which extracellular enzyme lifetimes are too short to become profitable. That limit is difficult to quantify because enzyme lifetimes in any environment are poorly constrained (e.g., 13). Thus, it is plausible that extracellular enzyme-mediated carbon acquisition is impractical in sediments in which metabolic rates are particularly slow.

While extracellular enzyme activity in surface sediments has frequently been reported, few reports exist of extracellular enzyme activity from deeper than 20 cm below the seafloor (cmbsf; 14). Enzyme activity has been reported in sapropels up to 389 cmbsf in sapropels in the Eastern Mediterranean Sea (15, 16) and in sediment from 600-630 cmbsf in Aarhus Bay sediments (17), as well as in a few other subsurface environments, such as the interior of seafloor basalts at the Loihi seamount (18). Furthermore, an analysis of transcriptomes from subsurface sediments of the Peru Margin revealed diverse exported peptidases and carbohydrate-active enzymes, which decreased in relative abundance with increasing depth (19).

101 In order to better understand how heterotrophic microorganisms in subsurface
102 sediments access organic matter, we assayed a diverse set of peptidases (protein-
103 degrading enzymes) in sediment cores from the White Oak River estuary, NC. We paired
104 these assays with analysis of the potential for extracellular peptidase production from
105 existing metagenomic data sets. We chose this site because the porewater geochemistry
106 and microbiology of these sediments has been well-characterized (20–24) and because
107 they contain abundant Bathyarchaeota and Thermoprofundales archaea, which appear to
108 be capable of metabolizing detrital organic matter (17, 25–27). We focused on
109 peptidases because protein degradation appears to be an important metabolism for some
110 subsurface archaea (17) and because peptidases were more active than other enzymes in
111 similar environments (15, 18). Because environmental samples contain a wide range of
112 distinct peptidases at variable activities (28, 29) we measured the hydrolysis of eleven
113 different substrates, which may be hydrolyzed by structurally and genetically diverse
114 extracellular peptidases.

115 Results

116 PEPTIDASE KINETICS

117 Sediment cores were sampled on two dates: first, to measure saturation curves for
118 six structurally diverse peptidase substrates, and second to measure a more targeted set of
119 peptidases at high depth resolution in order to assess the relative ability of subsurface
120 communities to access more degraded organic matter. Combining all samples,
121 unambiguous hydrolysis of nine different peptidase substrates was observed. All

122 peptidase substrates assayed with the more-sensitive single-cuvette methodology were
123 hydrolyzed much faster in untreated sediments than in autoclaved controls (Fig 1).
124 Kinetics of substrate hydrolysis were qualitatively consistent with the Michaelis-Menten
125 rate law, $v_0 = \frac{V_{max} \times [S]}{K_m + [S]}$, with estimated V_{max} values ranging from 40 to 3400 nmol g^{-1}
126 sediment hr^{-1} (median 310, interquartile range 190 to 560 nmol g^{-1} sediment hr^{-1}).
127 Throughout the core, AAF-AMC, GGR-AMC, and Gly-AMC were hydrolyzed the
128 fastest, and Arg-AMC was hydrolyzed slowest (Fig 2). Summed V_{max} values for each
129 substrate, a proxy for the total peptidolytic potential of the microbial community,
130 decreased with depth from 9.09 μmol AMC g^{-1} sed hr^{-1} at the surface to 1.24 μmol AMC
131 g^{-1} sed hr^{-1}, or 13% of the surface value, at 82.5 cmbsf. Estimated K_m values ranged from
132 36.1 μM to 1310 μM (median 138 μM, interquartile range 102 to 326 μM), and trended
133 downward (i.e., to greater substrate affinity) with increasing depth (Fig 3). K_m values for
134 hydrolysis of Leu-AMC were the greatest (i.e., lowest substrate affinity) while K_m values
135 for hydrolysis of BocVPR-AMC, GGR-AMC, and Arg-AMC were the least.
136 In a separate core, hydrolysis rates of D-Phe-AMC, L-Phe-AMC, and L-Orn-
137 AMC were assessed. These were measured using a plate-reader technique that proved
138 insufficiently precise to accurately measure V_{max} or K_m, so we have only reported the
139 observed hydrolysis rate v_0, which was measured at a high substrate concentration (400
140 μM) and therefore approximates V_{max}. Ratios of v_0 for D-Phe-AMC : L-Phe-AMC
141 hydrolysis and L-Orn-AMC : L-Phe-AMC hydrolysis rates increased approximately
142 linearly downcore (Fig 4).

MICROBIAL ABUNDANCE, CELL-SPECIFIC PEPTIDASE ACTIVITY, AND ORGANIC CARBON OXIDATION RATES

Concordantly with potential activities (Fig 5a), cell counts decreased more-or-less steadily downcore from 4.5×10^8 cells ml^{-1} wet sediment at 1.5 cmbsf to 7.4×10^7 cells ml^{-1} wet sediment at 82.5 cmbsf. Consequently, cell-specific total potential peptidase activity was roughly constant at 32 +/- 14 amol AMC $cell^{-1}$ hr^{-1} (Fig 5b) with no significant trend as a function of depth. Most of the error in cell-specific peptidase activities results from variance in cell counts rather than in V_{max} estimations.

Organic carbon oxidation rates were estimated using a 2-G model driven by porewater methane and sulfate concentrations. The total modeled organic carbon oxidation rate G at 82.5 cmbsf was approximately 0.17% relative to that at 4.5 cmbsf (the top of the model domain), a decrease of almost 3 orders of magnitude (Fig 5c). Thus, summed V_{max} relative to G, a proxy for the effort microbes exert compared to obtain complex organic carbon relative the amount of carbon they metabolize, increased more than 200-fold in the deepest sediments relative to surface sediments (Fig 5d).

PEPTIDASE GENES AND MICROBIAL TAXA

Samples for genomic analysis were taken from three broad sedimentary zones: the sulfate reduction zone (SRZ, 8-12 cmbsf), sulfate-methane transition zone (SMTZ, two distinct samples from nearby locations, 24-32 cmbsf and 26-30 cmbsf), and the methane-rich zone (52-54 cmbsf; data originally published in Baker *et al.*, 2015). A total of 3739 genes encoding extracellular peptidases were identified among metagenomes from the three depth zones examined, including 685 from SRZ, 1994 from SMTZ, and 1060 from

165 MRZ. Of the genes encoding for peptidases, 0-71% (depending on class of peptidase,
166 algorithm and sediment depth) contained a signal peptide (SP) and are likely secreted by
167 the SEC-dependent transport system (supplementary data). Among the genes associated
168 with signal peptides, members of peptidase family C25, belonging to the gingipain
169 family, were by far the most abundant at all depths, accounting for 41-45% of all SP-
170 associated peptidases (Fig. 6a). Genes annotated as encoding extracellular methionine
171 aminopeptidases and zinc carboxypeptidases were also abundant (13%-19%). Together,
172 these peptidase classes accounted for 73%, 76%, and 73% of exported peptidases in the
173 SRZ, SMTZ, and MRZ respectively. The composition of protein families was generally
174 consistent with depth, particularly among the more-abundant peptidases. Five peptidase
175 annotations were an exception to this trend: peptidase family M1, peptidase family
176 M20/M25/M40, peptidase family M3, M61 glycyl aminopeptidase, and thermophilic
177 metalloprotease (M29) were found in much lower abundance at the SMTZ than the MRZ
178 or SRZ. Given that those correspond to differences of one or a few total reads, these are
179 well within the range of noise.

180 *Proteobacteria* were by far the most abundant phylum in the SRZ sediments, with
181 smaller contributions from *Chloroflexi*, *Bacteroidetes*, *Planctomycetes*, *Euryarchaeota*,
182 and *Bathyarchaeota* (Fig 6b). This community differed substantially from the
183 communities in the SMTZ and MRZ, which were fairly similar to each other. In both
184 sediment depths, *Bathyarchaeota*, *Chloroflexi*, and *Proteobacteria* were the dominant
185 phyla.

186 ## Discussion

187 IDENTITIES OF EXTRACELLULAR PEPTIDASES PRESENT IN WHITE OAK RIVER
188 ESTUARY SEDIMENTS

189 Kinetics of fluorogenic substrate hydrolysis was consistent with the Michaelis-
190 Menten rate law and hydrolysis rates were dramatically slower in autoclaved controls
191 than in "live" treatments, indicating that the substrates were hydrolyzed by enzymes
192 rather than by abiotic factors. The enzyme substrates used here encompassed a diverse
193 range of amino acid and peptide chemistries, including polar and non-polar R groups at
194 the P1 site (i.e., the amino acid N-terminal to the scissile bond) and substrates with and
195 without steric protecting groups, which must have been hydrolyzed by endopeptidases
196 (which cleave proteins from within) and aminopeptidases (which cleave proteins from the
197 N terminus) respectively. Peptide bonds adjacent to a diverse set of amino acid residues
198 were cleaved, including glycine (the smallest amino acid), phenylalanine (among the
199 largest amino acids), arginine (positively charged at porewater pH) and leucine
200 (uncharged, hydrophobic), consistent with the presence of a diverse range of extracellular
201 peptidases throughout the core.

202 The metagenomic results also indicated the potential for a diverse range of
203 secreted peptidases, produced by a broad range of taxa, throughout the sediment column
204 (Fig 6). The metagenomic results represent a minimum estimate for the genomic potential
205 for extracellular peptidase production, because they rely on the assumption that only
206 those peptidases associated with signal peptides (SPs) are secreted. Non-SP-based
207 enzyme secretion pathways may also contribute to the pool of extracellular enzymes,

208 including Sec-independent secretion systems (30) and release of internal enzymes into
209 the extracellular medium by viral lysis (31, 32).
210 The dominance of genes for exported gingipain-like endopeptidases (class C25) at
211 all depths is consistent with rapid hydrolysis rates of fluorogenic substrates for
212 endopeptidases. Gingipains are endopeptidases with preference for arginine at the P1
213 position (i.e., the N-terminal side of the hydrolyzed bond), which would be active
214 towards the substrates GGR-AMC and Boc-VPR-AMC. Those were among the fastest-
215 hydrolyzed substrates at each depth (Figs. 1, 2), indicating that genes for C25 peptidases
216 were likely expressed. Previously, gingipains have been identified in Thermoprofundales
217 (formerly Marine Benthic Group D) and in Bathyarchaeota, and appear to be widespread
218 in marine sediments (17, 19, 33). The M28 family, also among the most abundant
219 annotations, contains a diverse range of aminopeptidases and carboxypeptidases
220 including leucine aminopeptidase, consistent with the observed hydrolysis of Leu-AMC
221 (34). Genes for D-aminopeptidases genes were observed, consistent with hydrolysis of D-
222 Phe-AMC.
223 Other abundant genes were annotated as methionine aminopeptidase, zinc
224 carboxypeptidase, a C-terminal domain from bacterial pre-peptidases, and peptidases
225 from the MEROPS families M24, S24, M50, and M28. Potential activities of these
226 peptidases were not assayed. Zinc carboxypeptidases (M20) cleave enzymes from the
227 carboxy-terminus and have strong specificity for Gly at the P1 position (i.e., the position
228 C-terminal to the scissile bond), but little preference for the residue at the P1' position
229 (the position C-terminal to the scissile bond; in a carboxypeptidase this would be the C-

230 terminus of the protein). Methionine aminopeptidases (M24) are metallopeptidases with
231 preference for glycine at the P1 position.
232 S24 and M50 peptidases are less likely to be directly relevant to organic matter
233 processing. S24 peptidases are involved in the SOS response for single-stranded DNA
234 repair (34). M50 peptidases are membrane-bound enzymes that act as sporulation factors
235 in Bacillus subtilis, and possibly other Bacteria (35, 36), and which are not secreted.
236 However, DNA repair (37, 38) and spore formation (39, 40) both appear to be important
237 survival mechanisms for microorganisms in subsurface sediments. The bacterial C-
238 terminal pre-peptidase domain is often found in secreted peptidases, but is removed prior
239 the peptidase becoming active, and could be associated with a wide range of peptidases
240 (41).
241 Each of these annotations is plausible in terms of what is known about peptidase
242 activities in sediments, and the annotations were generally consistent with the observed
243 activities. We did not assay for carboxypeptidases (e.g. MEROPS family M20) or
244 methionine aminopeptidase, but carboxypeptidases have previously been observed to be
245 active in estuarine sediments (42) and the generally broad substrate specificities of
246 extracellular aminopeptidases suggests that methionine aminopeptidases could have
247 contributed to the hydrolysis of the other aminopeptidase substrates (43). However, a
248 note of caution is also warranted when interpreting peptidase annotations from deeply
249 branching microorganisms: the high diversity of hydrolases makes precise annotations
250 difficult, and the exact substrate specificities of the peptidases in these samples may
251 differ somewhat from those inferred from the annotations (44). Thus, while these

252 annotations are environmentally plausible and generally consistent with the fluorogenic
253 enzyme assays, they should nevertheless be viewed with some skepticism.
254 Interestingly, the sets of peptidases identified in genomes, and the activities
255 observed, varied among depths much less than the microbes present (compare the similar
256 profiles in Fig 6a to the notable differences among depths in 6b.) It is possible that
257 extracellular enzymes were only produced by a small subset of taxa that are present at all
258 sediment depths, although this would be inconsistent with previous evidence that diverse
259 taxa including sulfate reducers and fermenters produce extracellular enzymes in
260 sediments (albeit, deeper than those studied here, 19), the widespread phylogenetic
261 distribution of similar extracellular enzymes (45), and previous observations of functional
262 redundancy with respect to extracellular enzyme production in diverse systems (46–48).

263 PEPTIDASE KINETICS SUGGEST ADAPTAION OF SUBSURFACE PEPTIDASES TO
264 DEGRADED ORGANIC MATTER

265 Heterotrophic microorganisms in subsurface sediments have little access to fresh
266 organic matter. In the cores described here, which represented ~275 years of sediment
267 deposition, organic matter oxidation rate decreased by at least three orders of magnitude
268 between the surface and 82.5 cmbsf (Fig 5c). It is challenging to determine what fraction
269 of high- vs low-molecular weight organic matter subsurface microorganisms metabolize.
270 However, the fact that cell-specific V_{max} was more-or-less constant downcore (Fig 5b)
271 suggests that the heterotrophic community relied on complex organic matter to a similar
272 degree at all depths. The cell-specific V_{max} values for Leu-AMC hydrolysis, 21-51 amol
273 cell^{-1} hr^{-1}, are comparable to previous measurements in active environments such as

surface sediments (2-100 amol $cell^{-1}$ hr^{-1}) and seawater (mostly less than 100 amol $cell^{-1}$ hr^{-1}, but with some measurements up to 10 nmol $cell^{-1}$ hr^{-1}; Vetter and Deming, 1994 and references therein), consistent with communities that relied primarily on organic carbon derived from macromolecules.

The ratio of ΣV_{max} : OC oxidation rate is sensitive to the mix of enzymes included in the sum, and to the substrate specificity of enzymes assayed (some enzymes will be capable of hydrolyzing multiple substrates). The absolute value of that sum, therefore, is not particularly meaningful. The trend, however, is informative: as sediment depth increased, the potential activity of extracellular peptidases decreased much more slowly than the actual rate of organic carbon oxidation, so the ratio of ΣV_{max} : OC oxidation rate increased dramatically (Fig 5d). V_{max} is a proxy for enzyme concentration, so the observed increase in ΣV_{max} : OC oxidation rate combined with the trend in cell-specific ΣV_{max} suggests that deeper heterotrophic communities exhibited similar demand for detrital OM, but that those enzymes returned bioavailable hydrolysate at a much slower rate because substrate concentrations were lower. The White Oak River subsurface communities were similar to their surface counterparts in terms of reliance on extracellular enzymes for bioavailable organic carbon, although subsurface metabolisms were considerably slower. However, enzyme kinetics and potential activities of D-phenylalanine aminopeptidase, L-phenylalanine aminopeptidase, and L-ornithine aminopeptidase all suggested microbial community adaptation to old, degraded organic matter in deeper sediments.

295 Most amino acids are biosynthesized as L-stereoisomers. As organic matter ages,
296 the ratio of D-amino acids to L-amino acids (D:L ratio) increases with depth, due to
297 abiotic racemization and increased abundance of D-amino acids derived from bacterial
298 cell walls (1, 50). Accordingly, the potential activity of D-phenylalanyl aminopeptidase
299 increased relative to that of L-phenylalanyl aminopeptidase, indicating an increased
300 capacity to access degraded organic matter. Ornithine, which is a product of the release of
301 urea from arginine, is another marker for degraded organic matter, while phenylalanine is
302 more characteristic of fresher organic matter (51), and the relative potential activity of L-
303 phenylalanine aminopeptidase : ornithine aminopeptidase followed the same increasing
304 trend with depth. Finally, the decrease of K_m values with increasing depth indicates
305 peptidases that function more efficiently at lower substrate concentrations. It is intuitive
306 that the concentration of enzyme-labile organic matter concentrations would decrease
307 downcore, and the observed increase in ΣV_{max} : OC oxidation rate provides direct
308 evidence of that. Taken together, these three observations provide strong evidence for a
309 subsurface heterotrophic microbial community that is increasingly adapted to persist
310 using degraded organic matter at increasing depth.
311 This evidence raises the ecological question of *how* selective pressure produces a
312 heterotrophic community adapted to degraded organic matter. Modeling and genomic
313 observations in older (thousands to millions of years), deeper sediments suggest that
314 microbial growth rates are too slow for community adaptation by enhanced growth rates
315 of more successful taxa; rather, communities in deeper sediments consist of taxa that
316 were deposited at the sediment-water interface and died at the slowest rates (6, 52, 53).

If those findings can be generalized to the shallower environments investigated here, that poses a question: in which aquatic environments are microorganisms capable gaining reproductive advantage by growing on recalcitrant organic carbon? The studies cited above addressed sites at which sedimentation rates, microbial respiration, and likely cell doubling times were considerably slower than in the sediments described here, so even if growth (as opposed to persistence) on recalcitrant organic carbon is not possible in those environments, it may have been in the White Oak River sediments. Alternately, microbial taxa may gain adaptations to metabolize recalcitrant organic matter in environments where labile organic matter is more abundant and growth rates are higher. This scenario would imply that organisms which primarily metabolize more labile organic matter would gain some selective advantage by also metabolizing recalcitrant organic matter. Finally, it is not entirely clear how the microorganisms in this study used the amino acids resulting from extracellular hydrolysis. In deeper sediments, heterotrophs appear to be energy-limited rather than carbon limited (54), which would suggest that amino acids would be likely assimilated directly into proteins. However, if amino acids are catabolized, there may be an energetic advantage to incorporating D-amino acids: some catabolic pathways for L-amino acids involve conversion to the D-form prior to further processing, in which case uptake of D-amino acids could save energy (55). Further analysis of the mechanisms by which subsurface heterotrophs access degraded sedimentary organic matter may yield insights into how microorganisms survive in low-energy environments, and into the processes that shape the pool of organic carbon that is preserved or oxidized over geological timescales.

Materials and Methods

STUDY SITE

Samples were collected from Station H in the White Oak River Estuary, 34° 44.490' N, 77° 07.44' W, first described by Gruebel and Martens (56). The White Oak River Estuary occupies a drowned river valley in the coastal plain of North Carolina. Station H is characterized by salinity in the range of 10 to 28 and water depth on the order of 2 m (21). The flux of ΣCO_2 across the sediment-water interface was 0.46 ± 0.02 mmol m^{-2} hr^{-1} (measured in May of 1987), primarily due to organic carbon oxidation via sulfate reduction. The sediment accumulation rate averages 0.3 cm yr^{-1}. Total organic carbon content is approximately 5% (21). For this study, push cores of 40-85 cm were collected from Station H by swimmers on May 28, 2013, and October 22, 2014. In 2013, cores were transported to the nearby Institute of Marine Sciences (University of North Carolina) at Morehead City, where they were sectioned and processed for enzyme activities, porewater geochemistry, and cell counts within 6 hours of sample collection. Porewater sulfate in 2013 was depleted by 43.5 cm, and methane peaked at 79.5 cm (Fig. S1). In 2014, cores were transported on the day of sampling to the University of Tennessee, Knoxville, stored at 4 °C, and processed for enzyme activities the following day. Samples for metagenomic analysis were collected separately in October 2010 from three sites (sites 1, 2, and 3, as previously described by Baker et al., 2015), all of which are within 550 m of Station H. Porewater geochemistry of those samples is described in

360 Figure S2 of Lazar et al (57). We note that, although the samples for sequencing were
361 taken at a different time and slightly different location than the samples for enzyme
362 assays, geochemistry and geomicrobiology of White Oak River sediments appears to be
363 extremely stable and homogenous, possibly due to the fact that sediments are extremely
364 fine and the estuarine water flow rates are low. In any case, geochemistry of the
365 sediments are stable over timescales of decades (21, 24, 58) and microbial abundances in
366 the SMTZ were very similar even though they were collected at sites separated by ~500m
367 (error bars in Fig 6b are mostly smaller than the differences among depths).

368 ENZYME ASSAYS

369 Enzyme assays were performed using different protocols in 2013 (data presented
370 in Figs 1-3) versus 2014 (data presented in Fig 4). In 2013, enzyme assays were
371 performed according to a protocol similar to the one described in Lloyd et al (2013b).
372 Cores were sectioned into 3 cm intervals. The following intervals were selected for
373 enzyme assays: 0-3 cm, 3-6 cm, 27-30 cm, 57-60 cm, and 81-83 cm. Each section was
374 homogenized, and approximately 0.5 ml wet sediment was transferred into separate 5 ml
375 amber glass serum vials, which had been pre-weighed and preloaded with 4 ml anoxic
376 artificial seawater (Sigma Sea Salts, salinity = 15, pH=7.5) Samples were weighed again
377 to determine the precise mass of wet sediment added, and then an appropriate quantity of
378 20 mM peptidase substrate stock dissolved in DMSO was added, up to 90 μL, for final
379 substrate concentrations of 0, 25, 50, 75, 100, 200, or 300 μM. Substrates are listed in
380 Table 1. Triplicate incubations with 400 μM Arg-AMC, Gly-AMC, Leu-AMC and Gly-
381 Gly-Arg-AMC were also created, but these were omitted for Ala-Ala-Phe-AMC and Boc-

382 Phe-Val-Arg-AMC because the latter two substrates are considerably more expensive.
383 Each serum vial was vortexed, briefly gassed with N_2 to remove oxygen introduced with
384 the sample, and approximately 1.3 ml slurry was immediately removed, transferred to a
385 microcentrifuge tube, and placed on ice to quench the reaction. The precise time of
386 quenching was recorded. This was centrifuged at 10,000 × *g* within approximately 15
387 minutes. The supernatant was transferred to a methacrylate cuvette and fluorescence was
388 measured with a Turner Biosystems TBS-380 fluorescence detector set to UV mode
389 (λ_{ex}=365-395 nm, λ_{em}=465-485 nm). Samples were then incubated at 16 °C,
390 approximately the *in situ* temperature, and the sampling procedure was repeated after
391 approximately 3 hours. The rate of fluorescence production was calculated as the increase
392 in fluorescence for each sample divided by the elapsed time between sample quenching.
393 Killed controls were made using homogenized, autoclaved sediments from 35-45 cmbsf.
394 However, we note that autoclaving does not completely destroy sediment enzymes
395 because sorption to mineral surfaces stabilizes enzyme structure, vastly increasing their
396 ability to maintain a functional conformation at high temperatures (59–61). We therefore
397 used the autoclaved samples as a qualitative control for the null hypothesis that enzymes
398 were responsible for none of the observed substrate hydrolysis, rather than as a
399 quantitative method to distinguish enzymatic substrate hydrolysis from potential abiotic
400 effects. In some sediments, a large fraction of fluorophore can sorb to particles, requiring
401 a correction to observed fluorescence (15, 16). In order to test the extent of sorption, we
402 incubated 120 nM AMC in WOR sediment slurry (12.5 g sediment / 100 mL ASW, pH =
403 7.5) over the course of 125 hours. Fluorescence was stable over the entire incubation (Fig

404 S2). Further, we sometimes measured fluorescence calibration curves repeatedly over ~3
405 hours, and observed no clear changes in the slopes of the curves. We thus concluded that
406 sorption of the free fluorophore was negligible.

407 In 2014, enzymes were assayed using a protocol based on the approach of Bell et
408 al (2013), which was designed for soil enzyme assays. In this approach, peptidase
409 substrates were mixed with sediment-buffer slurries in 2-mL wells of a deep-well plate.
410 These plates were periodically centrifuged and 250 μL aliquots of supernatant were
411 transferred into a black 96-well microplate. Fluorescence was read using a BioTek
412 Cytation 3 microplate reader (λ_{ex} = 360 nm, λ_{em} = 440 nm). Results from this method
413 proved considerably noisier than the single-cuvette method used in 2013, so kinetic
414 parameters (V_{max} and K_m) were not calculated for these data. Nevertheless, results were
415 qualitatively similar to those from 2013, and we have reported V_{max} from 2014 as v_0
416 measured at 400 μM substrate concentration, which was saturating. In October 2014, the
417 following substrates were assayed: AAF-AMC, Arg-AMC, Boc-VPR-AMC, D-Phe-
418 AMC, Gly-AMC, Leu-AMC, L-Phe-AMC, Orn-AMC, Z-Phe-Arg-AMC, and Z-Phe-Val-
419 Arg-AMC. In October 2014, L-Phe-AMC, D-Phe-AMC, and Orn-AMC were assayed
420 according to the same protocol in 3-cm core sections at 1.5, 4.5, 7.5, 10.5, 19.5, 22.5,
421 25.5, 28.5, 34.5, 37.5, 40.5, 43.5, 49.5, 52.5, 58.5, and 61.5 cmbsf.

422 Peptidase kinetic data were analyzed using R. All raw data and scripts related to
423 enzyme analysis are posted at http://github.com/adsteen/WOR_enz_2013_2014. For
424 samples taken using the more sensitive single-cuvette method, Michaelis-Menten
425 parameters were estimated from nonlinear least squares fits to kinetic data. In the case of

Leu-AMC at 4.5 centimeters below seafloor, kinetic data could not successfully be fit to a Michaelis-Menten function, so no K_m was reported and the value of v_0 at the highest substrate concentration was substituted for V_{max}. For analysis of correlations, data sets were qualitatively evaluated for homoskedasticity and normality of residuals using q-q plots and plots of residuals vs fitted values. When untransformed data met those criteria, the null hypothesis of no correlation was tested using linear least-squares regressions. When untransformed data failed to meet those criteria, data were log-transformed. In cases in which log-transformed data were either heteroskedastic or residuals were non-normally distributed, data were rank-transformed and correlations were tested using Spearman's ρ.

GEOCHEMICAL AND MICROBIOLOGICAL MEASUREMENTS

Sediment porosity was measured by mass after drying at 80 °C, according to the equation

$$\phi = \frac{m_w/\rho_w}{m_w/\rho_w + \frac{m_d - S \times m_w/1000}{\rho_{ds}}}$$

Here, m_w represents mass lost after drying, ρ_w represents the density of pure water, m_d represents the mass of the dry sediment, S represents salinity in g kg^{-1}, and ρ_{ds} represents the density of dry sediment (assumed to be 2.5 g cm^{-3}). Porewater sulfate concentrations were measured using a Dionex Ion Chromatograph (Sunnyvale, CA) in porewater that was separated by centrifugation in 15 ml centrifuge tubes at 5000 × *g* for 5

minutes, filtered at 0.2 μm, and acidified with 10% HCl. Methane was measured using 3 ml sediment subsamples that were collected from a cutoff syringe, entering through the side of a core section, immediately after core extrusion. Subsamples were deposited immediately in a 20 ml serum vial containing 1 ml, 0.1 M KOH. These were immediately stoppered and shaken to mix sediment with KOH. Methane was later measured by injecting 500 μl of bottle headspace into a GC-FID (Agilent, Santa Clara, CA) using a headspace equilibrium method (63).

GEOCHEMICAL MODELING

Organic carbon remineralization rates as a function of depth were estimated by applying a multi-component reaction-transport model to depth distributions of sulfate and methane concentration. The model is based on equations described in Boudreau (64) and includes only sulfate reduction and methane production due to lack of data regarding oxic and suboxic processes. Thus, the model is limited to depths greater than 4.5 cm where sulfate reduction and methane production are the dominant processes, and bioirrigation and bioturbation may be assumed to be negligible. The organic matter remineralization rate is parameterized using the multi-*G* model first proposed by Jørgensen (65); a two-component model was sufficient to accurately simulate the sulfate and methane data. For solutes, the upper boundary conditions were measured values at 4.5 cm while the lower boundary conditions (200 cm) were set to zero-gradient. The flux of reactive organic carbon to 4.5 cm was calculated from the sulfate flux across the 4.5 cm horizon and an estimate of methane burial below the lower boundary (the methane flux at the upper boundary was observed to be zero), with an assumed oxidation state of reactive carbon of

468 -0.7. The model contains four adjustable parameters that are set to capture the major
469 details of measured sulfate and methane data: first-order rate constants for both fractions
470 of the reactive carbon pool; the partitioning factor for both fractions, and the rate constant
471 for methane oxidation.

472 CELL ENUMERATION

473 Cells were enumerated by direct microscopic counts. One mL of sediment was
474 placed in a 2-mL screw-cap tube with 500 µl of 3% paraformaldehyde in phosphate
475 buffered saline (PBS), in which it was incubated overnight before being centrifuged for 5
476 minutes at 3000 × *g*. The supernatant was removed and replaced with 500 µl of PBS,
477 vortexed briefly and centrifuged again at 3000 × *g*. The supernatant was subsequently
478 removed and replaced with a 1:1 PBS:ethanol solution. Sediments were then sonicated
479 using a Branson Ultrasonics Sonifier SFX150 at 20% power for 40 seconds to
480 disaggregates cells from sediments and diluted 40-fold into PBS prior to filtration onto a
481 0.2 µm polycarbonate filter (Fisher Scientific, Waltham, MA) and mounted onto a slide.
482 Cells were stained with 4',6-diamidino-2-phenylindole (DAPI) and enumerated by direct
483 counts using a Leica Epifluorescence Microscope.

484 METAGENOMIC ANALYSIS

485 To resolve the taxonomic distribution of extracellular peptidases we searched a
486 pre-existing White Oak River *de novo* assembled and binned metagenomic dataset (Table
487 S2; Baker *et al.*, 2015) for genes that were assigned extracellular peptidase functions.
488 These assignments were based on best matches to extracellular peptidases in KEGG,

489 pfam, and NCBI-nr (non-redundant) databases using the IMG annotation pipeline
490 (Markowitz et al., 2014). Genes were additionally screened for signal peptidase motifs
491 using the following programs: PrediSI setting the organism group to gram-negative
492 bacteria (66), PRED-Signal trained on archaea (67), the standalone version of PSORT
493 v.3.0 trained against archaea (68), and SignalP 4.1 using gram-negative bacteria as the
494 organism group (69). All programs were used with default settings if not stated
495 otherwise. Binned genomes from three different depth zones of White Oak River
496 sediments were examined. The sulfate-rich zone (SRZ) genomes were obtained from sites
497 2 and 3 core sections 8-12 and 8-10 cm, respectively. The sulfate-methane transitions
498 zone (SMTZ) genomes were recovered from site 2 and 3 and depths of 30-32 cm and 24-
499 28 cm. The methane-rich zone (MRZ) was from site 1 and 52-54 cm. To determine
500 abundance of phyla, we used the 16S rRNA gene sequences that were automatically
501 extracted from the Baker et al metagenomes by IMG/m. We used CLC Genomic
502 Workbench 10.0 (CLC Bio, Aarhus, Denmark) to trim adaptors and make contigs from
503 bidirectional sequences. We clustered operational taxonomic units (OTUs) at 97%
504 similarity used Silva reference set 132 to identify the taxonomy of OTUs (70).
505

Acknowledgements

We thank Michael Piehler for access to his laboratory facilities at the University of North Carolina Institute of Marine Sciences, the captain of the R/V Capricorn for sampling assistance, and Terry Hazen for use of lab equipment at the University of Tennessee. We greatly appreciate two anonymous reviewers, whose constructive comments substantially improved the manuscript. Oliver Jeffers reminds ADS that science is cool and worth doing. Funding for KHM was provided by NSF grant DBI-1156644 to Steven W. Wilhelm. Funding for ADS was provided by NSF grant OCE-1431598 and a C-DEBI subaward. This work is C-DEBI Contribution number <<to be determined.>>

Conflict of interest

The authors declare no competing financial interests in relation to the work described.

522 ## References

523 1. Lomstein BA, Niggemann J, Jørgensen BB, Langerhuus AT. 2009. Accumulation
524 of prokaryotic remains during organic matter diagenesis in surface sediments off
525 Peru. Limnol Oceanogr 54:1139–1151.
526 2. Jørgensen BB, Marshall IPG. 2016. Slow Microbial Life in the Seabed. Ann Rev
527 Mar Sci 8:311–32.
528 3. Biddle JF, Lipp JS, Lever MA, Lloyd KG, Sørensen KB, Anderson R, Fredricks
529 HF, Elvert M, Kelly TJ, Schrag DP, Sogin ML, Brenchley JE, Teske A, House
530 CH, Hinrichs K-UK-U, Sorensen KB, Anderson R, Fredricks HF, Elvert M, Kelly
531 TJ, Schrag DP, Sogin ML, Brenchley JE, Teske A, House CH, Hinrichs K-UK-U.
532 2006. Heterotrophic Archaea dominate sedimentary subsurface ecosystems off
533 Peru. Proc Natl Acad Sci U S A 103:3846–51.
534 4. Hoehler TM, Jørgensen BB. 2013. Microbial life under extreme energy limitation.
535 Nat Rev Microbiol 11:83–94.
536 5. Lloyd KG, Steen AD, Ladau J, Yin J, Crosby L. 2018. Phylogenetically Novel
537 Uncultured Microbial Cells Dominate Earth Microbiomes. mSystems 3:e00055-
538 18.
539 6. Orsi WD. 2018. Ecology and evolution of seafloor and subseafloor microbial
540 communities. Nat Rev Microbiol 16:671–683.
541 7. Benz R, Bauer K. 1988. Permeation of hydrophilic molecules through the outer
542 membrane of gram-negative bacteria. Review on bacterial porins. Eur J Biochem
543 176:1–19.

544 8. Benner R, Amon RMW. 2015. The size-reactivity continuum of major bioelements
545 in the ocean. Ann Rev Mar Sci 7:185–205.
546 9. Reintjes G, Arnosti C, Fuchs BM, Amann R. 2017. An alternative polysaccharide
547 uptake mechanism of marine bacteria. ISME J 11:1640–1650.
548 10. Vetter YAY, Deming JJW, Jumars PPA, Krieger-Brockett BBB. 1998. A
549 Predictive model of bacterial foraging by means of freely released extracellular
550 enzymes. Microb Ecol 36:75–92.
551 11. Allison SD. 2005. Cheaters, diffusion and nutrients constrain decomposition by
552 microbial enzymes in spatially structured environments. Ecol Lett 8:626–635.
553 12. Schimel JP, Weintraub MN. 2003. The implications of exoenzyme activity on
554 microbial carbon and nitrogen limitation in soil: a theoretical model. Soil Biol
555 Biochem 35:549–563.
556 13. Steen AD, Arnosti C. 2011. Long lifetimes of β-glucosidase, leucine
557 aminopeptidase, and phosphatase in Arctic seawater. Mar Chem 123:127–132.
558 14. Arnosti C, Bell C, Moorhead DLL, Sinsabaugh RLL, Steen ADD, Stromberger M,
559 Wallenstein M, Weintraub MNN. 2014. Extracellular enzymes in terrestrial,
560 freshwater, and marine environments: perspectives on system variability and
561 common research needs. Biogeochemistry 117:5–21.
562 15. Coolen MJL, Overmann J. 2000. Functional exoenzymes as indicators of
563 metabolically active bacteria in 124,000-Year-old sapropel layers of the eastern
564 Mediterranean Sea. Appl Environ Microbiol 66:2589–2598.
565 16. Coolen MJL, Cypionka H, Sass AM, Sass H, Overmann J. 2002. Ongoing

566 modification of Mediterranean Pleistocene sapropels mediated by prokaryotes.
567 Science 296:2407–10.
568 17. Lloyd KGKG, Schreiber L, Petersen DGDG, Kjeldsen KUKU, Lever MAMA,
569 Steen AD, Stepanauskas R, Richter M, Kleindienst S, Lenk S, Schramm A,
570 Jørgensen BB, Jorgensen BB. 2013. Predominant archaea in marine sediments
571 degrade detrital proteins. Nature 496:215–8.
572 18. Meyers MEJ, Sylvan JB, Edwards KJ, Jacobson Meyers ME, Sylvan JB, Edwards
573 KJ. 2014. Extracellular enzyme activity and microbial diversity measured on
574 seafloor exposed basalts from Loihi seamount indicate the importance of basalts to
575 global biogeochemical cycling. Appl Environ Microbiol 80:4854–64.
576 19. Orsi WD, Richards TA, Francis WR. 2018. Predicted microbial secretomes and
577 their target substrates in marine sediment. Nat Microbiol 3:32–37.
578 20. Martens CS, Goldhaber MB. 1978. Early diagenesis in transitional sedimentary
579 environments of the White Oak River Estuary, North Carolina. Limnol Oceanogr
580 23:428–441.
581 21. Kelley CA, Martens CS, Chanton JPJP. 1990. Variations in sedimentary carbon
582 remineralization rates in the White Oak River estuary, North Carolina. Limnol
583 Oceanogr 35:372–383.
584 22. Baker BJ, Lazar CS, Teske AP, Dick GJ. 2015. Genomic resolution of linkages in
585 carbon, nitrogen, and sulfur cycling among widespread estuary sediment bacteria.
586 Microbiome 3:14.
587 23. Lazar CS, Baker BJ, Seitz K, Hyde AS, Dick GJ, Hinrichs K-U, Teske AP. 2016.

588 Genomic evidence for distinct carbon substrate preferences and ecological niches
589 of Bathyarchaeota in estuarine sediments. Environ Microbiol 18:1200–11.
590 24. Lloyd KG, Alperin MJ, Teske A. 2011. Environmental evidence for net methane
591 production and oxidation in putative ANaerobic MEthanotrophic (ANME)
592 archaea. Environ Microbiol 13:2548–2564.
593 25. Kubo K, Lloyd KG, F Biddle J, Amann R, Teske A, Knittel K. 2012. Archaea of
594 the Miscellaneous Crenarchaeotal Group are abundant, diverse and widespread in
595 marine sediments. ISME J 6:1949–65.
596 26. Meng J, Xu J, Qin D, He Y, Xiao X, Wang F. 2014. Genetic and functional
597 properties of uncultivated MCG archaea assessed by metagenome and gene
598 expression analyses. ISME J 8:650–9.
599 27. Zhou Z, Pan J, Wang F, Gu J-D, Li M. 2018. Bathyarchaeota: globally distributed
600 metabolic generalists in anoxic environments. FEMS Microbiol Rev 42:639–655.
601 28. Obayashi Y, Suzuki S. 2005. Proteolytic enzymes in coastal surface seawater:
602 Significant activity of endopeptidases and exopeptidases. Limnol Oceanogr
603 50:722–726.
604 29. Steen AD, Arnosti C. 2013. Extracellular peptidase and carbohydrate hydrolase
605 activities in an Arctic fjord (Smeerenburgfjord, Svalbard). Aquat Microb Ecol
606 69:93–99.
607 30. Bendtsen JD, Kiemer L, Fausbøll A, Brunak S. 2005. Non-classical protein
608 secretion in bacteria. BMC Microbiol 5:58.
609 31. Danovaro R, Dell'Anno A, Corinaldesi C, Magagnini M, Noble R, Tamburini C,

610 Weinbauer M. 2008. Major viral impact on the functioning of benthic deep-sea
611 ecosystems. Nature 454:1084–1087.
612 32. Breitbart M, Felts B, Kelley S, Mahaffy JM, Nulton J, Salamon P, Rohwer F.
613 2004. Diversity and population structure of a near-shore marine-sediment viral
614 community. Proc R Soc B Biol Sci 271:565–574.
615 33. Zhou Z, Liu Y, Lloyd KG, Pan J, Yang Y, Gu J-D, Li M. 2018. Genomic and
616 transcriptomic insights into the ecology and metabolism of benthic archaeal
617 cosmopolitan, Thermoprofundales (MBG-D archaea). ISME J 1.
618 34. Rawlings ND, Barrett AJ, Thomas PD, Huang X, Bateman A, Finn RD. 2018. The
619 MEROPS database of proteolytic enzymes, their substrates and inhibitors in 2017
620 and a comparison with peptidases in the PANTHER database. Nucleic Acids Res
621 46:D624–D632.
622 35. Green DH, Cutting SM. 2000. Membrane topology of the Bacillus subtilis pro-
623 sigma(K) processing complex. J Bacteriol 182:278–85.
624 36. Feng L, Yan H, Wu Z, Yan N, Wang Z, Jeffrey PD, Shi Y. 2007. Structure of a
625 site-2 protease family intramembrane metalloprotease. Science 318:1608–12.
626 37. Orsi WD, Edgcomb VP, Christman GD, Biddle JF. 2013. Gene expression in the
627 deep biosphere. Nature 499:205–208.
628 38. Bird JT, Tague E, Zinke L, Schmidt JM, Steen AD, Reese BK, Marshall I,
629 Webster G, Weightman A, Castro H, Campagna SR, Lloyd KG. Uncultured
630 microbial phyla suggest mechanisms for multi-thousand-year subsistence in Baltic
631 Sea sediments. MBio.

632 39. O'Sullivan LA, Roussel EG, Weightman AJ, Webster G, Hubert CR, Bell E, Head
633 I, Sass H, Parkes RJ. 2015. Survival of Desulfotomaculum spores from estuarine
634 sediments after serial autoclaving and high-temperature exposure. ISME J 9:922–
635 933.
636 40. Lomstein BA, Langerhuus AT, D'Hondt S, Jørgensen BB, Spivack AJ, D'Hondt
637 S, Jørgensen BB, Spivack AJ. 2012. Endospore abundance, microbial growth and
638 necromass turnover in deep sub-seafloor sediment. Nature 484:101–4.
639 41. Yeats C, Bentley S, Bateman A. 2003. New knowledge from old: in silico
640 discovery of novel protein domains in Streptomyces coelicolor. BMC Microbiol
641 3:3.
642 42. Pantoja S, Lee C, Marecek JF. 1997. Hydrolysis of peptides in seawater and
643 sediment. Mar Chem 57:25–40.
644 43. Steen AD, Vazin JPJP, Hagen SMSM, Mulligan KHKH, Wilhelm SWSW. 2015.
645 Substrate specificity of aquatic extracellular peptidases assessed by competitive
646 inhibition assays using synthetic substrates. Aquat Microb Ecol 75:271–281.
647 44. Michalska K, Steen AD, Chhor G, Endres M, Webber AT, Bird J, Lloyd KG,
648 Joachimiak A. 2015. New aminopeptidase from "microbial dark matter" archaeon.
649 FASEB J 29:4071–4079.
650 45. Zimmerman AE, Martiny AC, Allison SD. 2013. Microdiversity of extracellular
651 enzyme genes among sequenced prokaryotic genomes. ISME J 7:1187–1199.
652 46. Wohl DL, Arora S, Gladstone JR. 2004. Functional redundancy supports
653 biodiversity and ecosystem function in a closed and constant environment.

Ecology 85:1534–1540.

47. Reich PB, Walters MB, Ellsworth DS, Smith DP, Branco S, Glassman SI, Erlandson S, Vilgalys R, Liao H-L, Smith ME, Peay KG. 1997. From tropics to tundra: global convergence in plant functioning. Proc Natl Acad Sci U S A 94:13730–4.

48. Frossard A, Gerull L, Mutz M, Gessner MO. 2012. Disconnect of microbial structure and function: enzyme activities and bacterial communities in nascent stream corridors. ISME J 6:680–691.

49. Vetter YA, Deming JW. 1994. Extracellular enzyme activity in the Arctic Northeast Water polynya. Mar Ecol Prog Ser 114:23–34.

50. Bada JL, Luyendyk BP, Maynard JB. 1970. Marine sediments: Dating by the racemization of amino acids. Science (80-) 170:730–732.

51. Dauwe B, Middelburg JJ, Herman PMJ, Heip CHR. 1999. Linking diagenetic alteration of amino acids and bulk organic matter reactivity. Limnol Oceanogr 44:1809–1814.

52. Starnawski P, Bataillon T, Ettema TJG, Jochum LM, Schreiber L, Chen X, Lever MA, Polz MF, Jørgensen BB, Schramm A, Kjeldsen KU. 2017. Microbial community assembly and evolution in subseafloor sediment. Proc Natl Acad Sci 114.

53. Bradley JA, Amend JP, LaRowe DE. 2018. Survival of the fewest: Microbial dormancy and maintenance in marine sediments through deep time. Geobiology.

54. Morono Y, Terada T, Nishizawa M, Ito M, Hillion F, Takahata N, Sano Y, Inagaki

676 F. 2011. Carbon and nitrogen assimilation in deep subseafloor microbial cells.
677 Proc Natl Acad Sci 108:18295–18300.
678 55. Radkov AD, Moe LA. 2018. A Broad Spectrum Racemase in Pseudomonas putida
679 KT2440 Plays a Key Role in Amino Acid Catabolism. Front Microbiol 9:1343.
680 56. Gruebel KA, Martens CS. 1984. Radon-222 tracing of sediment-water chemical
681 transport in an estuarine sediment. Limnol Oceanogr 29:587–597.
682 57. Lazar CS, Baker BJ, Seitz K, Hyde AS, Dick GJ, Hinrichs K-U, Teske AP. 2016.
683 Genomic evidence for distinct carbon substrate preferences and ecological niches
684 of Bathyarchaeota in estuarine sediments. Environ Microbiol 18:1200–1211.
685 58. Benninger LK, Martens CS. 1983. Sources and fates of sedimentary organic matter
686 in the White Oak and Neuse River Estuaries.
687 59. Stursova M, Sinsabaugh RL. 2008. Stabilization of oxidative enzymes in desert
688 soil may limit organic matter accumulation. Soil Biol Biochem 40:550–553.
689 60. Carter DO, Yellowlees D, Tibbett M. 2007. Autoclaving kills soil microbes yet
690 soil enzymes remain active. Pedobiologia (Jena) 51:295–299.
691 61. Schmidt J. 2016. Microbial Extracellular Enzymes in Marine Sediments: Methods
692 Development and Potential Activities in the Baltic Sea Deep Biosphere. University
693 of Tennessee - Knoxville.
694 62. Bell CW, Fricks BE, Rocca JD, Steinweg JM, McMahon SK, Wallenstein MD.
695 2013. High-throughput fluorometric measurement of potential soil extracellular
696 enzyme activities. J Vis Exp e50961.
697 63. Lapham LL, Chanton JP, Martens CS, Sleeper K, Woolsey JR. 2008. Microbial

activity in surficial sediments overlying acoustic wipeout zones at a Gulf of Mexico cold seep. Geochemistry, Geophys Geosystems 9:Q06001.

64. Boudreau BP. 1996. A method-of-lines code for carbon and nutrient diagenesis in aquatic sediments. Comput Geosci 22:479–496.

65. Jørgensen BB, J⊘rgensen BB. 1978. A comparison of methods for the quantification of bacterial sulfate reduction in coastal marine sediments: II. Calculation from mathematical models. Geomicrobiol J 1:29–47.

66. Hiller K, Grote A, Scheer M, Münch R, Jahn D. 2004. PrediSi: Prediction of signal peptides and their cleavage positions. Nucleic Acids Res 32.

67. Bagos PG, Tsirigos KD, Plessas SK, Liakopoulos TD, Hamodrakas SJ. 2009. Prediction of signal peptides in archaea. Protein Eng Des Sel 22:27–35.

68. Yu NY, Wagner JR, Laird MR, Melli G, Rey S, Lo R, Dao P, Sahinalp SC, Ester M, Foster LJ, Brinkman FSL. 2010. PSORTb 3.0: improved protein subcellular localization prediction with refined localization subcategories and predictive capabilities for all prokaryotes. Bioinformatics 26:1608–1615.

69. Petersen TN, Brunak S, von Heijne G, Nielsen H. 2011. SignalP 4.0: discriminating signal peptides from transmembrane regions. Nat Methods 8:785–6.

70. Quast C, Pruesse E, Yilmaz P, Gerken J, Schweer T, Yarza P, Peplies J, Glöckner FO. 2012. The SILVA ribosomal RNA gene database project: improved data processing and web-based tools. Nucleic Acids Res 41:D590–D596.

720 ## Table

721 Table 1: Substrates used in this study and the enzymes that hydrolyze them. AMC stands
722 for aminomethylcoumarin, the moiety that becomes fluorescent after hydrolysis of the
723 peptide bond. All amino acids are in the L- stereoconformation unless otherwise noted.
724 Enzymes are described as "putative" because the substrate specificity of many
725 environmental peptidases is fairly broad, so multiple peptidases may hydrolyze any given
726 substrate.

Substrate	Abbreviation	Putative enzyme
L-arginine-7-amido-4-methylcoumarin	Arg-AMC	arginyl aminopeptidase
L-glycine-7-amido-4-methylcoumarin	Gly-AMC	glycyl aminopeptidase
L-leucine-7-amido-4-methylcoumarin	Leu-AMC	leucyl aminopeptidase
Carboxybenzoyl-glycine-glycine-arginine-7-amido-4-methylcoumarin	Z-GGR-AMC	gingipain and other endopeptidases
Alanine-alanine-phenylalanine-7-amido-4-methylcoumarine	AAF-AMC	clostripain and other endopeptidases
Boc-valine-proline-arginine-AMC	Boc-VPR-AMC	gingipain and other endopeptidases
D-phenylalanine-AMC	D-Phe-AMC	D-phenyalanine aminopeptidase
L-phenylalanine-AMC	L-Phe-AMC	L-phenylalanine-aminopeptidase
Ornithine-AMC	Orn-AMC	ornithine aminopeptidase

727

728

Figures and Legends

Figure 1: Saturation curves for six substrates measured using the single-cuvette reader methodology at each of six depths. Dark circles indicate "live" samples, open triangles indicate autoclaved controls. Lines indicate nonlinear least-squares fits to the Michaelis-Menten rate law. Substrate abbreviations are given in the column headings and are defined in Table 1. Sediment depths are listed on row headings in centimeters below sediment-water interface.

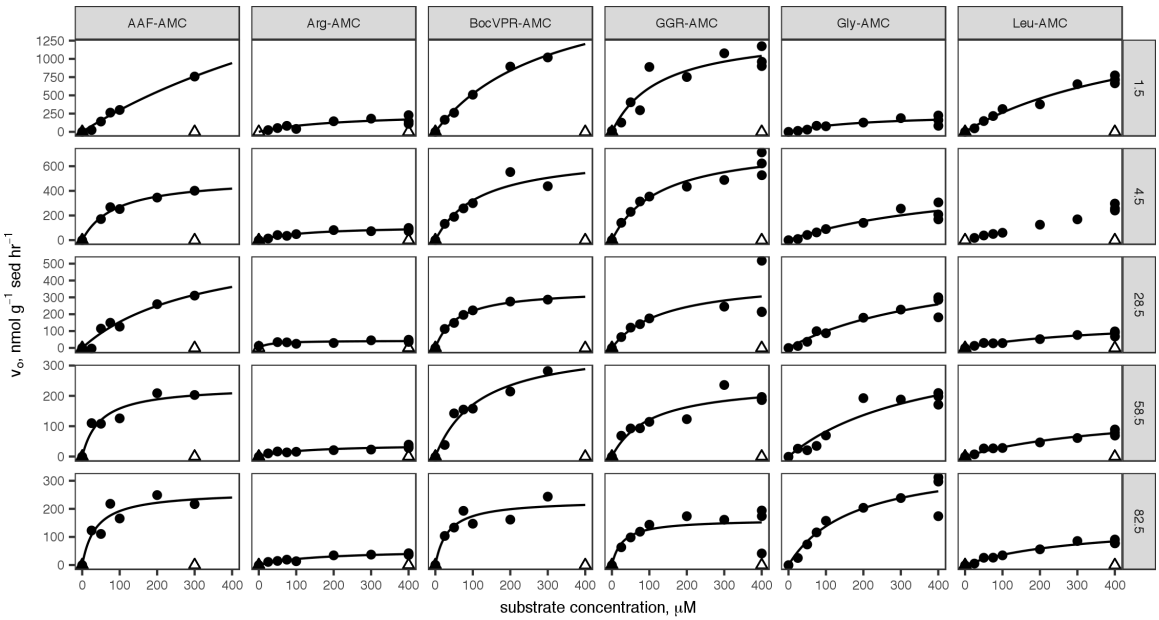

Fig 2: V_{max} and K_m values, shown individually with error bars indicating standard error of the nonlinear least-squares estimate, and collectively in a box-and-whiskers plot. Substrates sharing a letter are not significantly different according to one-way ANOVA of $\log_{10}$-transformed data with Tukey HSD post-hoc analysis (V_{max}), or Kruskal-Wallis test with Tukey HSD post-hoc analysis (K_m).

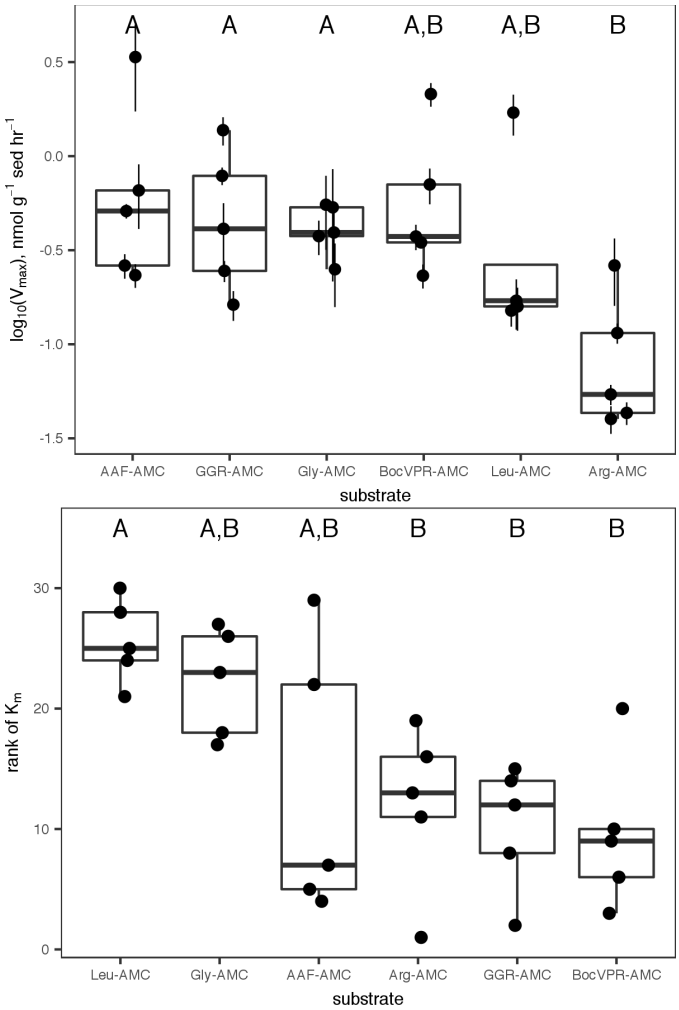

Fig 3: K_m values of extracellular peptidases as a function of depth. Details of substrates and the peptidases they correspond to are in Table 1. Error bars represent the standard deviation of replicate samples. Colored lines represent a linear least-squares regression for each substrate. The black line and gray shading represent linear regression and 95% confidence interval for all substrates taken together.

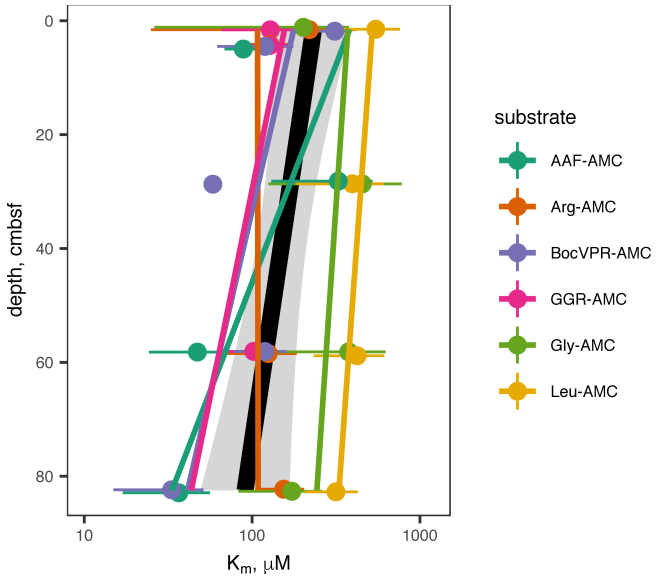

Fig 4: a.) Ratio of v_0 for D-phenylalanine aminopeptidase: L-phenylalanine aminopeptidase and b.) L-ornithine aminopeptidase : L-phenylalanine aminopeptidase. The linear regressions are given by D-Phe-AP:L-Phe-AP = 5.60 (± 1.87) × 10^{-3} × depth + 0.146 (± 0.067) and L-Orn-AP:L-Phe-AP = 2.26 (± 0.89) × 10^{-3} × depth + 0.451 (± 0.326)

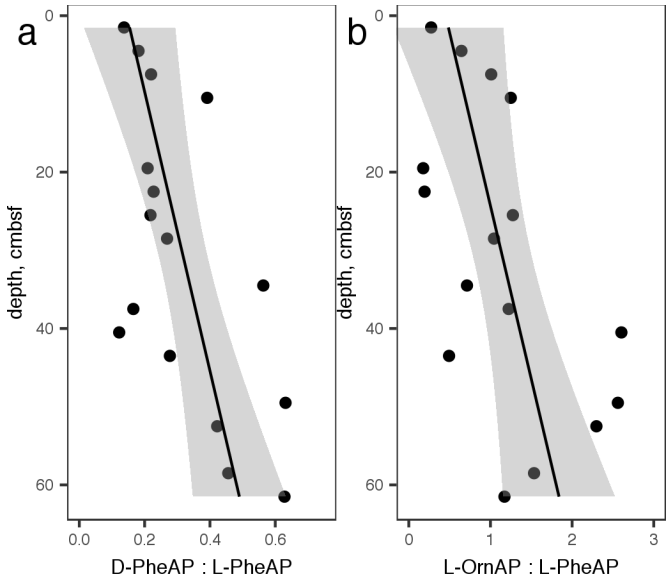

Figure 5: a.) The sum of all peptidase Vmax values, relative to the value at 4.5 cm, versus sediment depth. Error bars represent propagated error of the estimate of V_{max} for each substrate. b.) Summed V_{max} relative to cell count. Error bars represent propagated error from summed Vmax and cell counts, and is dominated by cell count uncertainty. c.) Organic carbon oxidation rates modeled from sulfate and methane profiles. d.) Summed V_{max} relative to modeled carbon oxidation rates. Error bars represent error in summed V_{max} relative to organic carbon oxidation rates, for which uncertainty was not modeled.

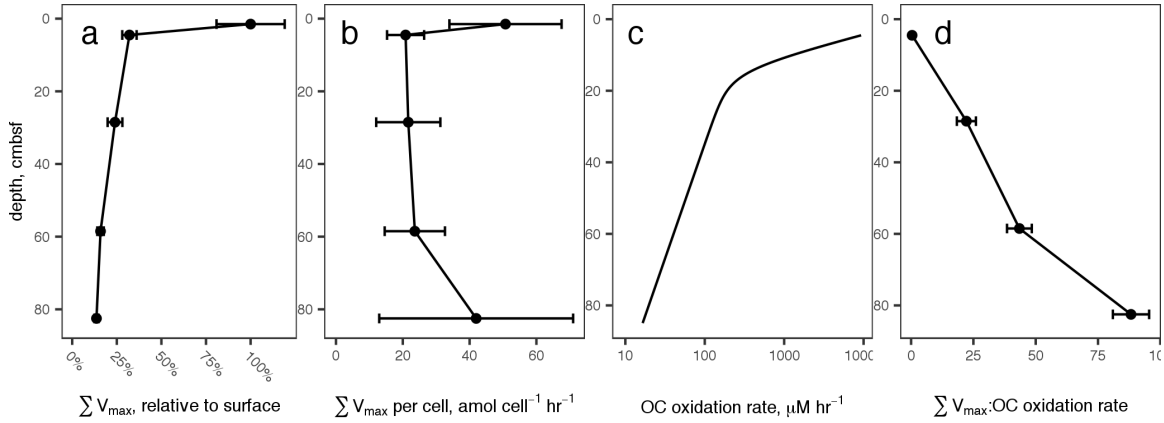

Fig 6: A.) Frequency of reads for genes of various classes of extracellular peptidases that were associated with signal peptidases, relative to all genes for extracellular peptidases at that depth. SRZ, SMTZ, and MRZ correspond to “sulfate reducing zone” (8-12 cmbsf), “sulfate-methane transition zone” (24-32 cmbsf) and “methane-rich zone” (24-28 cmbsf) respectively. B.) Relative abundance of phyla in bins at each depth. Only the 10 most abundant phyla at each depth are shown. The orange SMTZ points represent the average of two SMTZ samples, taken ~500 m apart from each other, and error bars represent the range of the two sites.

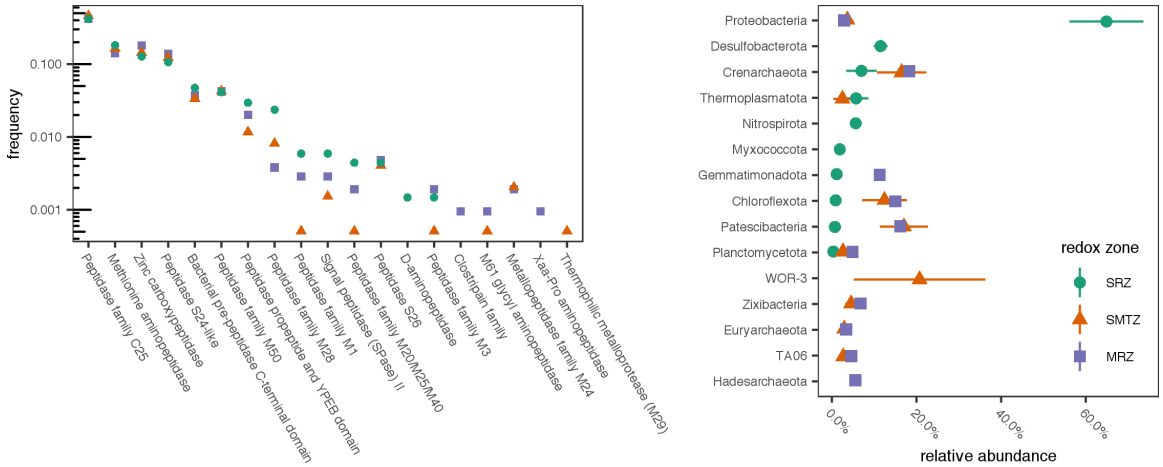

783 **Supplemental Information**

784 Supplemental file: annotations of all peptidases included in this manuscript.